Chalcogenide Letters Vol. 17, No. 6, June 2020, p. 321 - 328

OPTICAL AND ELECTRICAL STUDIES OF DOPED In-Se SYSTEM FOR PHASE-CHANGE MEMORY APPLICATIONS

M.D. SHARMA*, N. GOYAL
Department of Physics, Centre of Advanced Studies in Physics, Panjab University Chandigarh (160014), India

Chalcogenide glasses have gained popularity due to their optical and electrical properties and versatile applications in the field of science and technology. In this manuscript, we describe the preparation of antimony-doped Indium Selenide thin films with different concentrations of antimony. Structure and morphology of the prepared films are studied by X-ray diffraction and field-emission scanning electron microscope. The properties that are studied during this course of work include optical energy band gap, electrical properties, and dielectric measurements.

(Received March 14, 2020; Accepted June 19, 2020)

Keywords: Antimony, Indium, Selenium, Optical properties, Electrical properties

1. Introduction

Chalcogenide glasses, containing one or more chalcogens (S, Se, Te), are a topic of great interest among scientists. Owing to the intermediate energy band gap values, chalcogenide glasses are often called amorphous semiconductors which render them versatile applications in the field of electronic switching [1], memories [2] and photovoltaic applications [3], etc. These glasses exhibit optical transparency from visible to infrared regions which makes them suitable for use in optoelectronic applications [4], image storage [5], holography [6], optical amplifiers and optical emitters [7], xerography [8], infrared imaging and infrared detector [9].

Indium Selenide (InSe) is a novel system which is studied by the various group of scientists and is applicable in many fields of science and technology. Selenium is usually doped with other elements to enhance its properties like lifetime, sensitivity, conductivity, etc. Singh et al. [10]have prepared Se-In thin film by the conventional melt-quench technique and observed that the energy band gap decreases with increasing indium concentration and becomes constant after a particular concentration of indium. Spectral response of nanostructured InSe thin films recommends it to be a potential optical fiber material [11]. Darwish et al. [12] prepared bulk InSe by melt-quench technique and thin films were fabricated by thermal evaporation. Electrical properties like dielectric constant, dark electrical conductivity, Seebeck coefficient, etc were measured. With the increase in the thickness of the film, conductivity increases, and the Seebeck coefficient also depends on the thickness of the films. The ac conductivity follows the correlated barrier hopping model [13]. When illuminated with ultra-violet light, there is a change in the crystallite size and refractive index of the films [14] thus making InSe a potential material to be used for optical data storage. InSe films are also reported to be a suitable candidate for photovoltaic applications [15].

In our previous work [16], we have reported the preparation of lead doped In-Se films and studied their optical and electrical properties. In this manuscript, we present antimony doped In-Se films for phase change memory applications.

* Corresponding author: manishdevsharma@yahoo.com

2. Experimental details

2.1. Preparation of bulk material

Bulk samples of pure $In_{10}Se_{90}$ and Sb doped $(In_{10}Se_{90})_{100-x}Sb_x$ where x= (2, 5, 10) were prepared using the conventional melt-quench technique. Using an electronic balance, all the elements were weighted according to the proper stoichiometric compositions: $(In_{10}Se_{90})_{98}Sb_2$, $(In_{10}Se_{90})_{95}Sb_5$ and $(In_{10}Se_{90})_{90}Sb_{10}$. All the components in their powdered form were mixed and put in the quartz ampoules. While maintaining the vacuum of 10^{-5} mbar, the quartz ampoules were sealed from one end using glass blowing process. The ampoules were then put in a muffle furnace for 24 hours for homogeneous melting and mixing of constituent elements at an elevated temperature of 1000°C and immediately quenched in liquid Nitrogen. The glassy alloys thus obtained were further grounded to obtain the desired bulk samples.

2.2. Thin-film preparation

Thin films of the samples were obtained by thermal evaporation technique. The bulk samples were thermally evaporated in a Molybdenum (Mo) boat and were deposited on a clean glass plate(3 cm*3 cm). Throughout the process, the vacuum of 10^{-5} mbar was maintained using a diffusion pump. For the thermal stability of films, they are kept in vacuum unit overnight.

3. Results and discussion

Morphology, optical properties and electrical properties of the prepared thin films namely pure $In_{10}Se_{90}$, $(In_{10}Se_{90})_{98}Sb_2$, $(In_{10}Se_{90})_{95}Sb_5$ and $(In_{10}Se_{90})_{90}Sb_{10}$ were studied.

3.1. Structural characterization

3.1.1. X-Ray Diffraction

Energy dispersive X-Ray analysis reflects the presence of antimony in the prepared films (Table 1). X-ray diffraction of the samples was done using PANalyticalX'Pert Pro X-ray diffractometer with Cu-Kα source (λ= 1.54 Å).The diffractogram of pure $In_{10}Se_{90}$ is shown in Fig. 2(a). It is perceived that pure $In_{10}Se_{90}$ is amorphous and has only one peak at 2θ = 23.2°of(004) crystal plane of $In_{10}Se_{90}$. The average crystallite size comes out to be 14.7 nm. The d-spacing, calculated using Bragg's relation, corresponding to the crystalline peak 23.2° is found to be 3.83 Å.

Table 1. Composition of antimony doped InSe films.

	Elemental composition		
	In%	Se%	Sb%
$In_{10}Se_{90}$	11.59	88.43	-
$(In_{10}Se_{90})_{98}Sb_2$	11.23	87.07	1.70
$(In_{10}Se_{90})_{95}Sb_5$	9.00	86.10	4.91
$(In_{10}Se_{90})_{90}Sb_{10}$	10.83	80.49	8.64

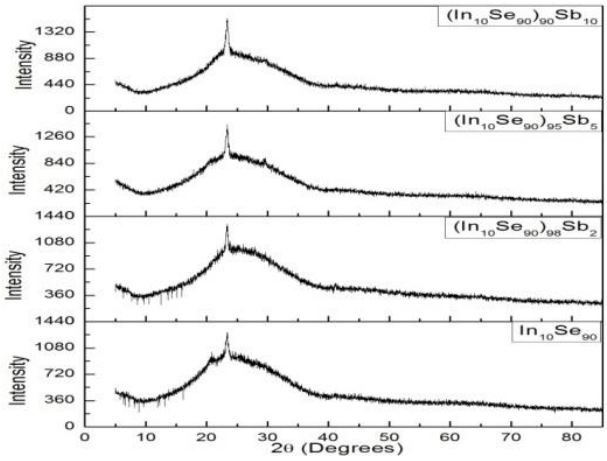

Fig. 1. X-ray graphs of pure In-Se and Sb-doped In-Se films.

With the incorporation of antimony, the characteristic peak is still observed at 23.2° indicating that no new phase is formed after the addition of Sb in $In_{10}Se_{90}$. But with an increase in the concentration of Sb, the intensity of the existing phase is enhanced as the intensity of the peak is increased as shown in Fig.1.

3.1.2. Field-Effect Scanning Electron Microscope

The shape of the particles and particle size is measured using HITACHI Field-Effect Scanning Electron Microscope (FE-SEM) SU-8010 model. The particles of pure $In_{10}Se_{90}$ are spherical and dimensions are of the order of nanometer (Fig.2(a)). FE-SEM micrographs of $(In_{10}Se_{90})_{98}Sb_2$, $(In_{10}Se_{90})_{95}Sb_5$ and $(In_{10}Se_{90})_{90}Sb_{10}$ are shown in Fig. 2 (b)-(d). It is observed that with an increase in the concentration of Sb, the shape of the particles gets distorted and they grow in size. At 10 at wt. % of Sb, maximum agglomeration is observed.

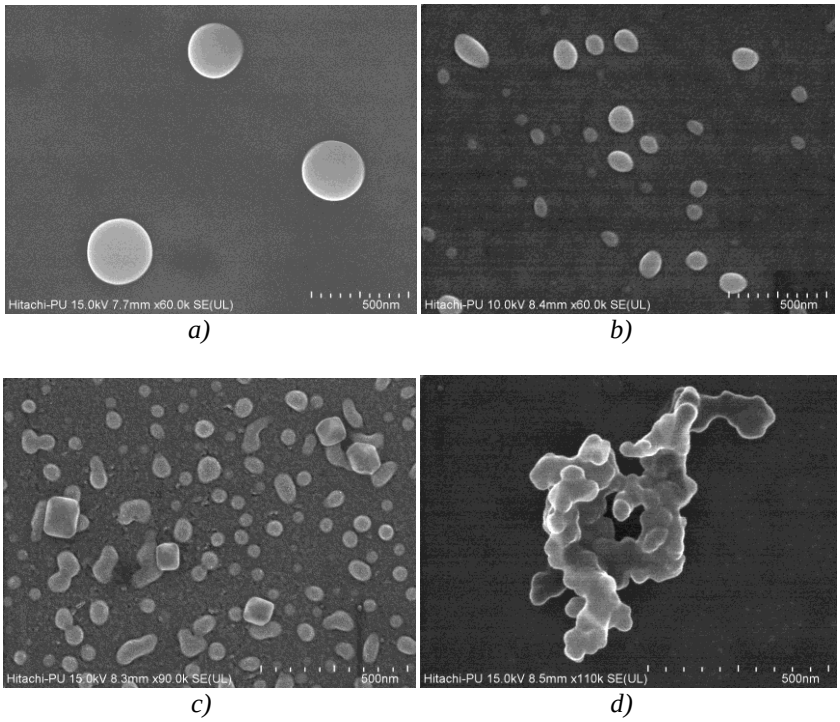

a) *b)*

c) *d)*

Fig.2. FESEM images of (a) Pure In-Se (b) $(In_{10}Se_{90})_{98}Sb_2$ (c) $(In_{10}Se_{90})_{95}Sb_5$ (d) $(In_{10}Se_{90})_{90}Sb_{10}$.

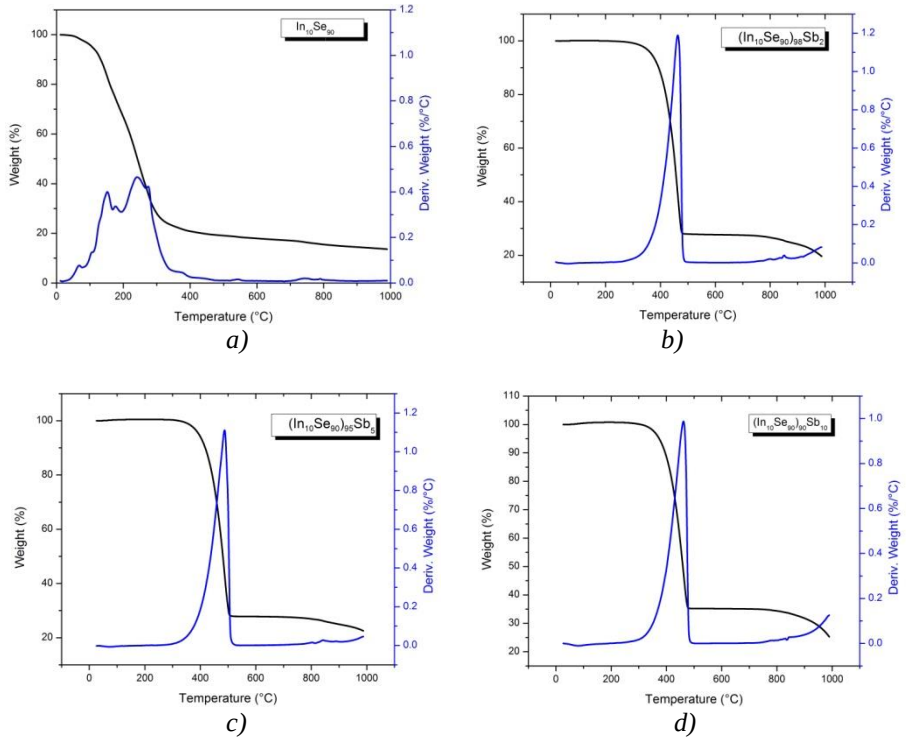

Fig.3. TGA and DSC curves of (a) Pure In-Se (b) $(In_{10}Se_{90})_{98}Sb_2$ (c) $(In_{10}Se_{90})_{95}Sb_5$ (d) $(In_{10}Se_{90})_{90}Sb_{10}$

3.2. Thermal study

3.2.1. Thermogravimetric Analysis and Differential Scanning Calorimetry

Pure $In_{10}Se_{90}$ films are stable up to a temperature of 170°C as indicated by the TGA and DSC curves (Fig. 3(a)). TGA and DSC curves for $(In_{10}Se_{90})_{98}Sb_2$, $(In_{10}Se_{90})_{95}Sb_5$ and $(In_{10}Se_{90})_{90}Sb_{10}$ are shown in Fig. 3(b)-(d). There is a remarkable increase in the degradation temperature of all the samples from 170°C to 400°C. The crystallization peak also copies the same temperature of crystallization.

3.3. Optical Characterization: UV-VIS Spectroscopy

The power law given by Tauc, which describes the correlation between the coefficient of absorption (α) and the energy of the incident photon (hν), is used to evaluate the bandgap of materials.The graph plotted between $(\alpha h\nu)^{1/n}$ vshν is used to find the value of the band gap when the linear portion of the graph is extrapolated to meet the abscissa. The Tauc plot for pure $In_{10}Se_{90}$, $(In_{10}Se_{90})_{98}Sb_2$, $(In_{10}Se_{90})_{95}Sb_5$ and $(In_{10}Se_{90})_{90}Sb_{10}$ are shown in Fig. 4 (a)-(d). From the plots, it is observed that with the change in the concentration of Sb, there is a change in the value of the band gap but the optical band gap of Sb doped $In_{10}Se_{90}$ films shows no particular trend. Variation in the value of the band gap is tabulated in Table 2.

Table 2. Band gap values corresponding to different concentrations of Sb.

S.No.	Material	Band gap (eV)
1.	$In_{10}Se_{90}$	1.50
2.	$(In_{10}Se_{90})_{98}Sb_2$	1.35
3.	$(In_{10}Se_{90})_{95}Sb_5$	1.53
4.	$(In_{10}Se_{90})_{90}Sb_{10}$	1.34

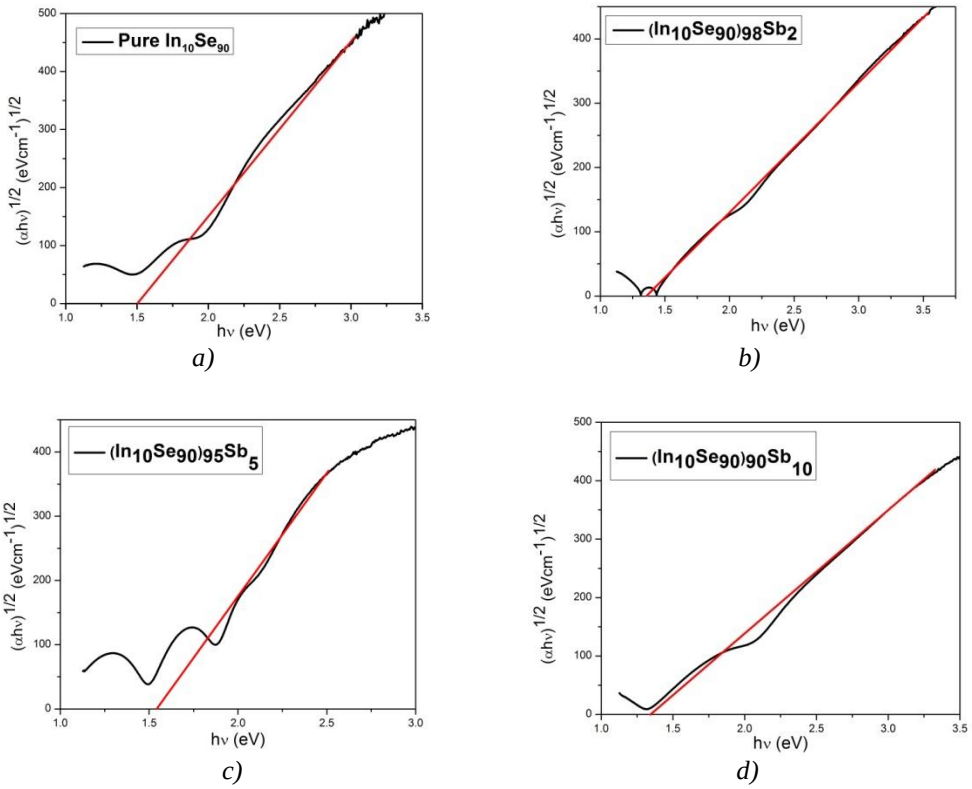

Fig. 4. Tauc plot of Sb-doped In-Se films.

3.4. Electrical study

The electrical properties were determined using two probe method with Keithley 6517A electrometer as a voltage source and DNM-121 nano-ammeter as a current measuring source in a sample holder connected to a rotary pump. The vacuum of 10^{-3} mbar is maintained throughout the experiments. Silver electrodes were deposited on the films of all the sample alloys to study the electrical behavior of the materials.

3.4.1. Current-Voltage Characterization

Using two probe process, Current-Voltage (I-V) characterization of all the samples were done to check for the ohmic response of the samples. For different values of voltage ranging from 0V to 5V, corresponding values of current were noted down. The I-V characteristics come out to be linear for pure $In_{10}Se_{90}$ and $(In_{10}Se_{90})_{98}Sb_2$, $(In_{10}Se_{90})_{95}Sb_5$ and $(In_{10}Se_{90})_{90}Sb_{10}$ (Fig. 5), which suggests the ohmic nature exhibited by all alloys.

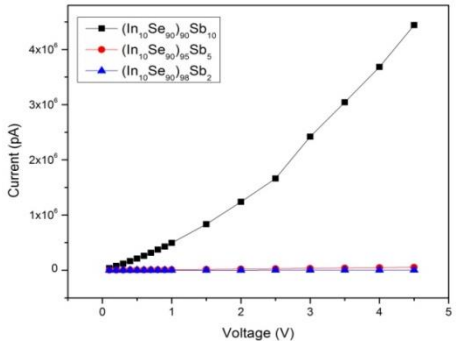

Fig. 5. Current-voltage characteristics of Sb-doped In-Se films.

3.4.2. Capacitance-Voltage (C-V) and Dielectric Measurement

The dielectric measurements were done for pure $In_{10}Se_{90}$ and Sb doped samples: $(In_{10}Se_{90})_{98}Sb_2$, $(In_{10}Se_{90})_{95}Sb_5$ and $(In_{10}Se_{90})_{90}Sb_{10}$ over the frequency ranging from 50Hz to 5MHz. Using LCR meter, Capacitance (C) and Conductance (G) were measured and using these values, various parameters were calculated like the real and imaginary part of dielectric constant (ε' and ε'' respectively) using the following relations:

$$\varepsilon' = \frac{C}{C_0} = \frac{Cd}{\varepsilon_0 A} \tag{1}$$

$$\varepsilon'' = \frac{G}{\omega C_0} = \frac{Gd}{\omega \varepsilon_0 A} \tag{2}$$

where C_0 is the capacitance of the empty capacitor, d and A arethe sample thickness (cm) and sample area (cm^2) respectively. The dielectric constantversus frequency graphs are shown in Figs. 6(a) and 6(b). It is spotted that with an increase in frequency both real and imaginary parts of dielectric constant are decreasing. However, thevalues of ε' and ε'' become stable at higher frequencies. This behavior of dielectric constant could be accounted for by Maxwell-Wagner and Koops[17]nomenological theory according to which inept conducting grains are separated from one another by several conducting grains. Grain boundaries play a crucial role at low frequency but at high frequency, conducting grains play a major role. At low frequencies, dielectric constant values are affected by the surface charge polarization. When the frequency increases, electrons are unable to keep in phase with applied electric field, thus lag behind the field. This electron lagging spreads over the entire domain; hence the value of dielectric constant decreases. An increase in the doping level of chalcogenide glasses leads to lower values of ε' and ε'' which may be due to the modification of defect states.

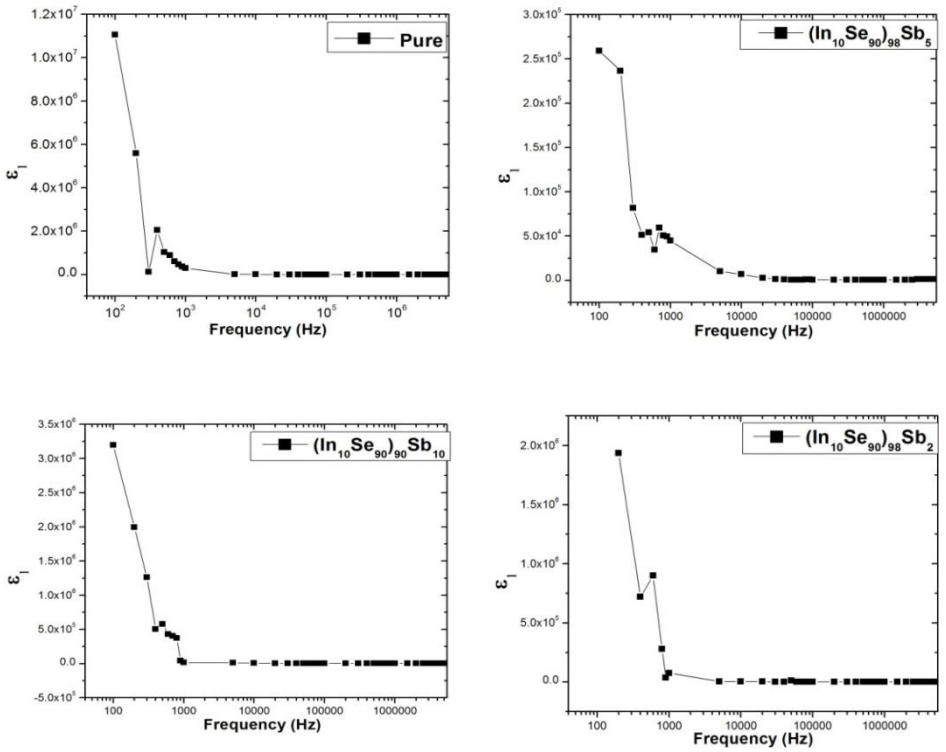

Fig. 6. (a) Real part of dielectric constant of Sb-doped In-Se films.

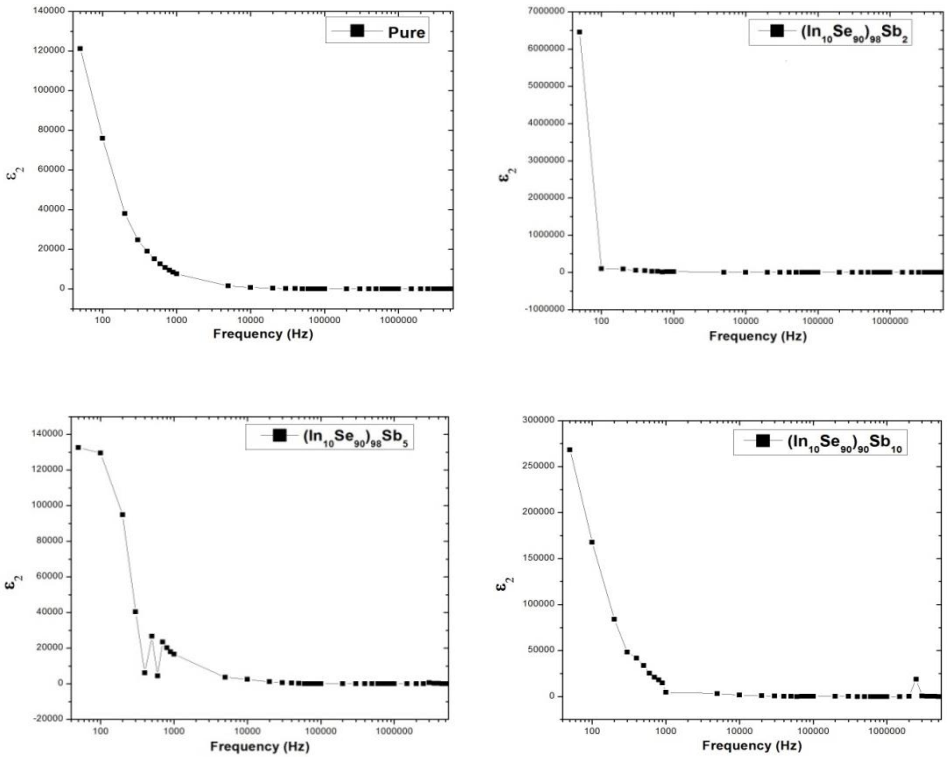

Fig. 6. (b) Imaginary part of dielectric constant of Sb-doped In-Se films.

4. Conclusions

In a nutshell, pure In-Se and Sb-doped In-Se films are fabricated using the melt-quench technique and thermal evaporation technique. The prepared films are amorphous and is justified by the X-ray diffractograms. With the incorporation of Sb, no new phase is formed but the intensity of the existing phase increases. TGA and DSC studies show that with increase in the concentration of Sb, the thermal stability of the films increases. The dielectric constant of the prepared films decreases with frequency and becomes constant at higher frequencies.

Acknowledgment

We are thankful to the Department of Physics, Panjab University, Chandigarh for providing us lab facilities and a healthy and peaceful environment to carry out this research work.

References

[1] S. R. Ovshinsky, Phys. Rev. Lett.**21**(20), 1450 (1968).
[2] T. Gille, K. De Meyer, D. J. Wouters, Phase Transitions**81**(7-8), 773 (2008).
[3] H. Noguchi, A. Setiyadi, H. Tanamura, T. Nagatomo, O. Omoto, Sol. Energy Mater. Sol. Cells**35**(C), 325 (1994).
[4] D. Lezal, J. Zavadil, M. Prochazka, Sulfide, Selenide and Telluride Glassy Systems for Optoelectronic Applications, 2005.
[5] A. G. Vedeshwar, Optical Storage Films, Chalcogenide Compound Films, in Encyclopedia of Smart Materials, John Wiley & Sons, Inc., 2002.
[6] J. Teteris, Curr. Opin. Solid State Mater. Sci.**7**(2), 127 (2003).
[7] E. Lupan, V. Ciornea, M. Iovu, Ge 25 Ga 1.7 As 8.3 S 65 Glass Doped with Pr 3+ FOR

1.3 μm Optical Amplifiers, 2009.
[8] G. Pfister, J. Electron. Mater.**8**(6), 789 (1979).
[9] A. Yang et al., J. Am. Ceram. Soc.**99**(1), 12 (2016).
[10] K. Singh, N. S. Saxena, O. N. Srivastava, D. Patidar, T. P. Sharma, Energy Band Gap Of Se 100-X In X Chalcogenide Glasses, 2006.
[11] M. M. El-Nahass, A. B. A. Saleh, A. A. A. Darwish, M. H. Bahlol, Opt. Commun.**285**(6), 1221 (2012).
[12] A. A. A. Darwish, M. M. El-Nahass, M. H. Bahlol, Appl. Surf. Sci.**276**, 210(2013).
[13] A. A. A. Darwish, M. M. El-Nahass, A. E. Bekheet, J. Alloys Compd.**586**, 142(2014).
[14] A. A. A. Darwish, Opt. Commun.**310**, 104 (2014).
[15] M. Teena, A. G. Kunjomana, K. Ramesh, R. Venkatesh, N. Naresh, Sol. Energy Mater. Sol. Cells**166**, 190 (2017).
[16] M. D. Sharma, N. Goyal, Applications of Advanced Electronic Materials: InSe SYSTEM (In 10 Se 90) 100-x Pb x With x = 0, 2, 5, 10 For Pcram Applications
[17] J. Bahadur, S. Agrawal, A. Parveen, A. Jawad, S. S. Z. Ashraf, R. M. Ghalib,Mater. Focus **4**(2), 134 (2015).